

ELLIPTIC ANALOGUE OF VERSHIK-KEROV LIMIT SHAPE

ANDREI GREKOV, NIKITA NEKRASOV

ABSTRACT. We review the limit shape problem for the Plancherel measure and its generalizations found in supersymmetric gauge theory instanton count. We focus on the measure, interpolating between the Plancherel measure and uniform measure, a $U(1)$ case of $\mathcal{N} = 2^*$ gauge theory. We give the formula for its limit shape in terms of elliptic functions, generalizing the trigonometric “arcsin” law of Vershik-Kerov and Logan-Schepp

Dedicated to the 90th anniversary of Anatoly Moiseevich Vershik,
with admiration

1. INTRODUCTION

In a seminal paper [6] A. Vershik and S. Kerov studied the large N asymptotics of the Plancherel measure on the set of irreducible representations R_λ of symmetric group $S(N)$:

$$(1) \quad \mu[\lambda] = \frac{(\dim R_\lambda)^2}{N!}$$

To R_λ one associates Young diagram λ

$$(2) \quad \lambda = (\lambda_i), \quad \lambda_1 \geq \lambda_2 \geq \dots \geq \lambda_{\ell(\lambda)} > 0$$

with

$$(3) \quad |\lambda| = N = \lambda_1 + \lambda_2 + \dots + \lambda_{\ell(\lambda)}$$

boxes. The main result of [6] is that upon rescaling the linear size of λ by \sqrt{N} one finds, in the $N \rightarrow \infty$ limit, a piecewise smooth curve $f(x)$, the *arcsin law*, which is read off a certain rational curve Σ through a solution of a Riemann-Hilbert problem. This limit shape curve determines the large N asymptotics of expectation values of all the moments (cf. [15])

$$(4) \quad \mathbf{p}_k[\lambda] = (1 - 2^{-k})\zeta(-k) + \sum_{i=1}^{\infty} \left(\lambda_i - i + \frac{1}{2} \right)^k - \left(-i + \frac{1}{2} \right)^k$$

Random Young diagrams behave in a way, similar to large N random $N \times N$ matrices.

In this small note we will study a one-parametric family of random partition models, motivated by the studies of supersymmetric gauge theories in four dimensions [11]. The measure (1) arises in a limit. To be more

precise, the original Vershik-Kerov problem can be equivalently studied in the macrocanonical ensemble, where one sums over all N with the weight $\frac{1}{N!}z^N$, with the parameter z called fugacity. Instead of the large N limit one studies the large z limit. It is this ensemble that we generalize below.

The paper is organized as follows. In section **2** we rederive the main result of [6] using the language of qq -characters [14, 13]. In section **3** we introduce our generalization of the macrocanonical ensemble, the corresponding qq -character. In section **4** we solve the limit shape problem by using the factorization of the *theta-transform* of the qq -character. In section **5** we discuss various limits of our solution: comparison to Vershik-Kerov limit shape, as well as the edge behavior. In section **6** we discuss future directions, including the *higher times* generalizations of the problem.

2. PROFILES, LIMIT SHAPES, THE ARCSIN LAW

We will use the results and notations from [11].

The Plancherel measure (1) above is a probability measure on the set of Young diagrams of fixed size N , as

$$(5) \quad \sum_{\lambda, |\lambda|=N} \mu[\lambda] = 1$$

In the studies of four dimensional gauge theory [12] one arrives at the similar measure, but defined on the set of all Young diagrams, the size $N = |\lambda|$ being weighted with a fugacity factor

$$(6) \quad \mu_{\Lambda, \hbar}(\lambda) = \frac{1}{Z} \frac{1}{N!} \left(\frac{i\Lambda}{\hbar} \right)^{2N} \mu[\lambda]$$

where the parameters Λ and \hbar have the meaning of the instanton counting parameter and the $SU(2)$ -rotation equivariant parameter, respectively. The normalization factor Z is given by:

$$(7) \quad Z = \sum_{\lambda} \left(\frac{i\Lambda}{\hbar} \right)^{2|\lambda|} \prod_{\square \in \lambda} \frac{1}{h_{\square}^2}$$

where h_{\square} - is a hook length of a box (i, j) in the Young diagram λ :

$$(8) \quad h_{i,j} = \lambda_i - j + \lambda_j^t - i + 1$$

Let x be an indeterminate. Define the $\mathbf{Y}(x)$ -observable on the set of all Young diagrams by

$$(9) \quad \mathbf{Y}(x)|_{\lambda} = x \prod_{\square \in \lambda} \frac{(x - \hbar c_{\square})^2 - \hbar^2}{(x - \hbar c_{\square})^2}$$

where for $\square = (i, j) \in \lambda$ its *content* is defined by

$$(10) \quad c_{i,j} = i - j$$

By cancellation of factors in the product it could be also written as:

$$(11) \quad \mathbf{Y}(x)|_\lambda = x \prod_{i=1}^{\ell_\lambda} \frac{x - \hbar i}{x + \hbar(\lambda_i - i)} \frac{x + \hbar(\lambda_i - i + 1)}{x + \hbar(1 - i)} = \frac{\prod_{\square \in \partial_+ \lambda} (x - \hbar c_\square)}{\prod_{\blacksquare \in \partial_- \lambda} (x - \hbar c_\blacksquare)}$$

where $\lambda_i = 0$ for $i > \ell_\lambda = \lambda_1^t$, and $\partial_+ \lambda$ and $\partial_- \lambda$ are the sets of boxes which can be added to or removed from λ , respectively.

Obviously, the expectation value

$$(12) \quad \langle \mathbf{Y}(x) \rangle := \sum_{\lambda} \mu_{\Lambda, \hbar}[\lambda] \mathbf{Y}(x)|_\lambda$$

has poles as a function of x . Define another observable, the *character*

$$(13) \quad \chi(x)|_\lambda = \mathbf{Y}(x)|_\lambda + \frac{\Lambda^2}{\mathbf{Y}(x)|_\lambda}$$

It was proven in [13], that the expectation value $\langle \chi(x) \rangle$ of the qq -character is pole-free. From (9), (13) we see that:

$$(14) \quad \mathbf{Y}(x), \chi(x) \sim x + O\left(\frac{1}{x^2}\right), \text{ as } x \rightarrow \infty$$

hence:

$$(15) \quad \langle \chi(x) \rangle = x$$

Now we are ready to apply the main result of [11]. Namely, in the limit $\hbar \rightarrow 0$, the correlation functions defined using the measure (6) factorize,

$$(16) \quad \langle \mathcal{O}_1 \mathcal{O}_2 \rangle = \langle \mathcal{O}_1 \rangle \langle \mathcal{O}_2 \rangle + o(\hbar), \quad \hbar \rightarrow 0$$

thus they become evaluations on the limit shape λ^∞ , defined as a C^0 limit $f(x)$ (in fact, the limit is in C^1) of the profile function $f_\lambda(x)$ (cf. [11]):

$$(17) \quad f_\lambda(x) := |x| + \sum_{i=1}^{\infty} (|x - \hbar(\lambda_i - i + 1)| - |x - \hbar(\lambda_i - i)| + |x + \hbar i| - |x + \hbar(i - 1)|) .$$

We give an example of profile $f_\lambda(x)$ below (1): The $\mathbf{Y}(x)$ -observable ex-

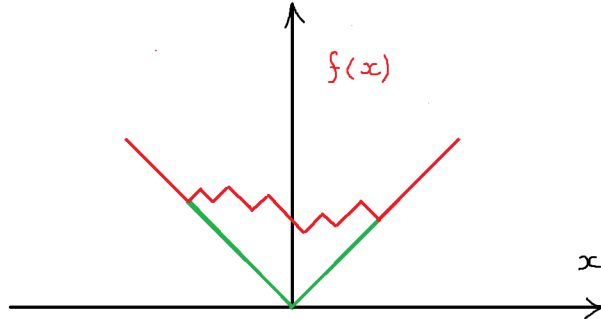


FIGURE 1. Young diagram profile function

presses through the profile function via [11]:

$$(18) \quad \mathbf{Y}(x)|_\lambda = \exp \left[\frac{1}{2} \int_{\mathbb{R}} \log(x-y) f''_\lambda(y) dy \right]$$

It follows from the formula (11) by direct calculation. The factorization (16) is proven using the standard argument [6]: the measure (6) scales as

$$(19) \quad \mu_{\Lambda, \hbar}(\lambda) = (1 + O(\hbar)) \times e^{\frac{1}{2\hbar^2} \text{P.V.} \int_{\mathbb{R}^2} dx_1 dx_2 f''_\lambda(x_1) f''_\lambda(x_2) (x_1 - x_2)^2 \left(\log\left(\frac{x_1 - x_2}{\Lambda}\right) - \frac{3}{2} \right)}$$

while the entropy factor, the number of configurations λ whose profile is C^0 -close to $f(x)$, grows as

$$(20) \quad \propto e^{c \frac{L_\lambda}{\hbar}}$$

where L_λ is a length of the boundary of λ , measured in \hbar -units, $L = \hbar(\lambda_1^t + \lambda_1)$, and c is a constant of order 1. Thus, in $\hbar \rightarrow 0$ limit

$$(21) \quad \langle \mathbf{Y}(x) \rangle \rightarrow Y(x), \quad \langle \mathbf{Y}(x)^{-1} \rangle \rightarrow \frac{1}{Y(x)}$$

with

$$(22) \quad Y(x) = \exp \left[\frac{1}{2} \int_{\mathbb{R}} \log(x-y) f''(y) dy \right]$$

so that (15) becomes the equation of the rational curve:

$$(23) \quad x = Y(x) + \frac{\Lambda^2}{Y(x)}$$

Taking the derivative of (22) one gets:

$$(24) \quad G(x) := \frac{d}{dx} \log Y(x) = \frac{1}{2} \int_{\mathbb{R}} \frac{f''(y)}{x-y} dy,$$

a function admitting analytic continuation to the complex plane $x \in \mathbb{C}$, with branch cut on the support of $f''(x)$. The jump of $G(x)$ across the cut is equal to:

$$(25) \quad G(x + i0) - G(x - i0) = i\pi f''(x)$$

To read off $f''(x)$ we compare the expression above to the solution of (23):

$$(26) \quad Y(x) = \frac{x}{2} + \frac{1}{2} \sqrt{x^2 - 4\Lambda^2}$$

The Eq. (23) has two solutions for $Y(x)$ in terms of x . The “+” branch of the square root in (26) is chosen so as to give the correct large x asymptotics (14). Taking the derivative we arrive at:

$$(27) \quad G(x) = \frac{1}{\sqrt{x^2 - 4\Lambda^2}}$$

It has a branch cut from -2Λ to 2Λ . Calculating the jump across it we arrive at the expression for $f''(x)$ (for $|x| < 2\Lambda$):

$$(28) \quad f''(x) = \frac{1}{\pi\Lambda} \frac{1}{\sqrt{1 - \left(\frac{x}{2\Lambda}\right)^2}}$$

The size of the corresponding partition asymptotes to

$$(29) \quad N \sim \frac{1}{4\hbar^2} \int_{\mathbb{R}} f''(x)x^2 = \frac{\Lambda^2}{2\hbar^2}$$

Integrating (28) once gives:

$$(30) \quad f'(x) = \frac{2}{\pi} \arcsin \frac{x}{2\Lambda}$$

and integrating twice we are proving the following theorem:

Theorem 2.1. (*Vershik-Kerov-Logan-Schepp'77*, [6, 8]) *The limit shape of the distribution (1) on the set of Young diagrams of size N as $\hbar \sim \frac{\Lambda}{\sqrt{2N}} \rightarrow 0$ is described by the following profile:*

$$(31) \quad f_{VK}(x) = \begin{cases} \frac{2}{\pi} \left(x \arcsin \frac{x}{2\Lambda} + \sqrt{4\Lambda^2 - x^2} \right), & |x| \leq 2\Lambda \\ |x|, & |x| \geq 2\Lambda \end{cases}$$

representing \hbar -rescaled piece-wise linear boundary of λ .

Remark. Mathematicians usually present (31) with $\Lambda = 1$. Keeping Λ as a parameter is motivated by generalizations involving, e.g. several random Young diagrams [12].

3. ELLIPTIC GENERALIZATION OF VERSHIK-KEROV MODEL

In this section we are introducing a one parameter deformation of (6). It arises in the studies of mass deformed maximally supersymmetric gauge theory, the so-called $\mathcal{N} = 2^*$ theory [12]:

$$(32) \quad \mu_{m,q,\hbar}[\lambda] = \frac{q^{|\lambda|}}{Z_{2^*}(m, q, \hbar)} \prod_{\square \in \lambda} \left(1 - \left(\frac{m}{\hbar h_{\square}} \right)^2 \right)$$

with the normalization partition function Z_{2^*} defined so that $\sum_{\lambda} \mu_{m,q,\hbar}[\lambda] = 1^1$. The fugacity

$$(33) \quad q = e^{2\pi i\tau}$$

is usually written in terms of the modular parameter

$$(34) \quad \tau = \frac{\vartheta}{2\pi} + \frac{4\pi i}{g^2}$$

of elliptic curve underlying the microscopic $\mathcal{N} = 4$ theory [3], in agreement with the Montonen-Olive S-duality conjecture [16]. Mathematically the measure makes sense for any complex values of m and q such that

¹In [11, 13] an explicit formula for Z_{2^*} can be found, but we don't need it here

$|\mathfrak{q}| < 1$, however in order for it to be a positive definite distribution on the set of all Young diagrams we restrict $\mathfrak{q} \in \mathbb{R}$, and $m \in i\mathbb{R}$.

The $\mathbf{Y}(x)$ -observable is defined as before by (9), while the qq -character is much more involved (cf. Eq. (153) in the arxiv version of [13], see also [14], where the $\hbar \rightarrow 0$ limit was analyzed):

$$(35) \quad \chi(x) = \sum_{\nu} \mu_{\hbar, \mathfrak{q}, m}[\nu] \frac{\prod_{\square \in \partial_{+\nu}} \mathbf{Y}(x + mc_{\square})}{\prod_{\square \in \partial_{-\nu}} \mathbf{Y}(x + mc_{\square})}.$$

In (35) the sum is taken over the set of auxiliary Young diagrams ν , not to be confused with the diagrams λ of the original ensemble (32). Note that the roles of m and \hbar in (35) are switched compared to (32).

The main theorem of [13] implies that the expectation value:

$$(36) \quad \langle \chi(x) \rangle_{2^*} := \sum_{\lambda} \mu_{m, \mathfrak{q}, \hbar}[\lambda] \chi(x)|_{\lambda}$$

has no poles in x , behaves as x for large x , therefore it is equal to x :

$$(37) \quad \langle \chi(x) \rangle_{2^*} = x.$$

4. SOLVING FOR LIMIT SHAPE IN THE ELLIPTIC CASE

In the limit $\hbar \rightarrow 0$, the same arguments as in the previous section show the expectation values of $\mathbf{Y}(x)$ tend to evaluations on the limit shape $\lambda_{2^*}^{\infty}$,

$$(38) \quad \langle \mathbf{Y}(x) \rangle_{2^*} \xrightarrow{\hbar \rightarrow 0} Y(x),$$

$$\langle \chi(x) \rangle_{2^*} \xrightarrow{\hbar \rightarrow 0} \phi(\mathfrak{q}) \sum_{\nu} \mathfrak{q}^{|\nu|} \frac{\prod_{\square \in \partial_{+\nu}} Y(x + mc_{\square})}{\prod_{\square \in \partial_{-\nu}} Y(x + mc_{\square})}$$

where

$$(39) \quad \phi(\mathfrak{q}) = \prod_{n=1}^{\infty} (1 - \mathfrak{q}^n).$$

Comparing (38) and (37) we get the functional equation:

$$(40) \quad \frac{x}{\phi(\mathfrak{q})} = \sum_{\nu} \mathfrak{q}^{|\nu|} \frac{\prod_{\square \in \partial_{+\nu}} Y(x + mc_{\square})}{\prod_{\square \in \partial_{-\nu}} Y(x + mc_{\square})}$$

for $Y(x)$, replacing the Eq. (23) of Vershik-Kerov problem. It would appear impossible to solve the infinite order non-linear difference equation Eq.(40). However it is solvable by what we call the θ -transform. Fix $z \in \mathbb{C}^{\times}$, spectral parameter in the world of integrable systems. Apply

$$(41) \quad \chi(x) \mapsto \sum_{n \in \mathbb{Z}} (-z)^n \mathfrak{q}^{\frac{n^2-n}{2}} \chi(x + mn) \quad \text{for } z \in \mathbb{C}^*$$

to both sides of the Eq. (40). Using factorization formula proven in the Appendix, one arrives at:

$$(42) \quad x\theta(z; \mathfrak{q}) + mz \frac{d}{dz} \theta(z; \mathfrak{q}) = \phi(\mathfrak{q})Y(x) \times \prod_{n=0}^{\infty} \left(1 - z\mathfrak{q}^n \frac{Y(x + (n+1)m)}{Y(x + nm)} \right) \prod_{n=1}^{\infty} \left(1 - z^{-1}\mathfrak{q}^n \frac{Y(x - nm)}{Y(x - (n-1)m)} \right)$$

where:

$$(43) \quad \theta(z; \mathfrak{q}) := \sum_{n \in \mathbb{Z}} (-z)^n \mathfrak{q}^{\frac{n^2-n}{2}} = (1-z) \prod_{n=1}^{\infty} (1 - \mathfrak{q}^n)(1 - z\mathfrak{q}^n)(1 - z^{-1}\mathfrak{q}^n)$$

By comparing the expressions for zeros of the LHS and the RHS of the equality above we will be able to express $Y(x)$ in terms of x as explicitly as needed to find the limit shape profile. Indeed, from the LHS we see that its zeros are described by (cf. [11] where this was derived by another method):

$$(44) \quad x = x(z) = -mz \frac{d}{dz} \log \theta(z; \mathfrak{q}) =$$

$$(45) \quad = m \left(\frac{z}{1-z} + \sum_{n=1}^{\infty} \left(\frac{z\mathfrak{q}^n}{1-z\mathfrak{q}^n} + \frac{\mathfrak{q}^n}{\mathfrak{q}^n - z} \right) \right)$$

As function of z , x obeys

$$(46) \quad x(\mathfrak{q}z) = x(z) + m$$

The real part of this function is depicted on figure (2) as a function of $\log z$. Define the fundamental cylinder to be the annulus $|\mathfrak{q}|^{1/2} < |z| < |\mathfrak{q}|^{-1/2}$. On

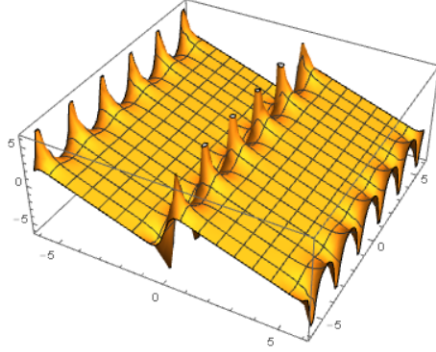


FIGURE 2. $\text{Re}[x(z)]$

the fundamental cylinder the inverse function $z(x)$ is well defined. To first order in \mathfrak{q} it looks like:

$$(47) \quad z(x) = \frac{1}{1 + \frac{m}{x}} + O(\mathfrak{q})$$

Hence we see that:

$$(48) \quad z(x = \infty) = 1$$

Now, let us have a look at the RHS of Eq. (42). We see that the set of its zeros is a curve, whose branches are labeled by integers:

$$(49) \quad z_n(x) = \mathfrak{q}^n \frac{Y(x - nm)}{Y(x + (1 - n)m)}, \quad n \in \mathbb{Z}$$

each behaving like:

$$(50) \quad z_n(x) \rightarrow \mathfrak{q}^n \quad \text{as } x \rightarrow \infty$$

In (47) we choose the $n = 0$ branch:

$$(51) \quad z(x) = z_0(x) = \frac{Y(x)}{Y(x + m)}$$

Thus, we obtain the identity:

$$(52) \quad \frac{d}{dx} \log z(x) = \frac{1}{2} \int_{\mathbb{R}} \frac{f''(y)}{x - y} dy - \frac{1}{2} \int_{\mathbb{R}} \frac{f''(y)}{x - y + m} dy$$

for the limit profile function $f \in C^1(\mathbb{R})$, which is related to $Y(x)$ as in (22). From this we derive:

$$(53) \quad \frac{d}{dx} \log z(x) = \frac{1}{z \frac{dx}{dz}} = \frac{1}{m F_{\mathfrak{q}}(z)}$$

where:

$$(54) \quad F_{\mathfrak{q}}(z) = \sum_{n \in \mathbb{Z}} \frac{z \mathfrak{q}^n}{(1 - z \mathfrak{q}^n)^2}$$

one gets:

$$(55) \quad \frac{1}{F_{\mathfrak{q}}(z(x))} = \frac{m}{2} \int_{\mathbb{R}} \frac{f''(y)}{x - y} dy - \frac{m}{2} \int_{\mathbb{R}} \frac{f''(y)}{x - y + m} dy$$

The RHS of Eq. (55) has, as a function of x , two branch cuts a distance m apart from each other, with the opposite sign jumps across each. As $x \rightarrow \infty$ the RHS of (55) goes to zero, as $(m/x)^2$, since

$$(56) \quad \int_{\mathbb{R}} f''(y) dy = 2$$

in agreement with the LHS.

The quasiperiodicity of $x(z)$ implies the branch cuts in the RHS correspond to the top and bottom edges of the fundamental cylinder in the z variable: $|z| = |\mathfrak{q}|^{1/2}$ and $|z| = |\mathfrak{q}|^{-1/2}$. Let us describe their locations explicitly.

For the bottom edge (parameterized by angle θ) one has:

$$(57) \quad x(\mathfrak{q}^{1/2} e^{i\theta}) = im \sin \theta g_{\mathfrak{q}}(\cos \theta)$$

where:

$$(58) \quad g_{\mathfrak{q}}(\cos \theta) = 2 \sum_{r \in \mathbb{Z}_{\geq 0 + \frac{1}{2}}} \frac{\mathfrak{q}^r}{1 - 2\mathfrak{q}^r \cos \theta + \mathfrak{q}^{2r}}$$

and for the upper edge we have:

$$(59) \quad x(\mathfrak{q}^{-1/2} e^{i\theta}) = x(\mathfrak{q}^{1/2} e^{i\theta}) - m$$

As $X(\theta) := -ix(\mathfrak{q}^{1/2} e^{i\theta})/m$ is real for $\theta \in [-\pi, \pi]$ (it is depicted approximately for $\mathfrak{q} = 1/3$ on figure (3)) we see that one branch cut is located on a real axis, and another one is shifted from it into the imaginary direction by $-m$. Since $X(\theta)$ is odd:

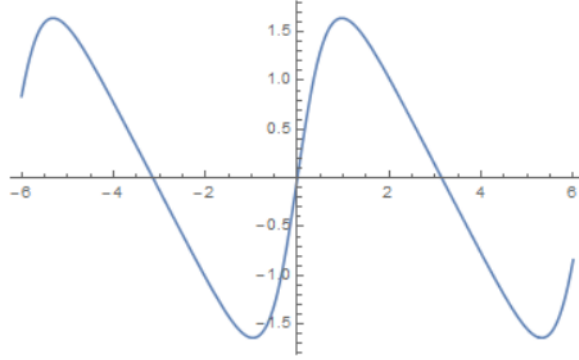


FIGURE 3. $X(\theta)$

$$(60) \quad X(-\theta) = -X(\theta),$$

it vanishes at $\theta = 0$ and $\theta = \pi$, therefore it has a maximum $\theta_* \in (0, \pi)$:

$$(61) \quad X'(\theta_*) = 0.$$

From the Eq. (65) below it follows it is unique. Accordingly, $\pm x_*$, with

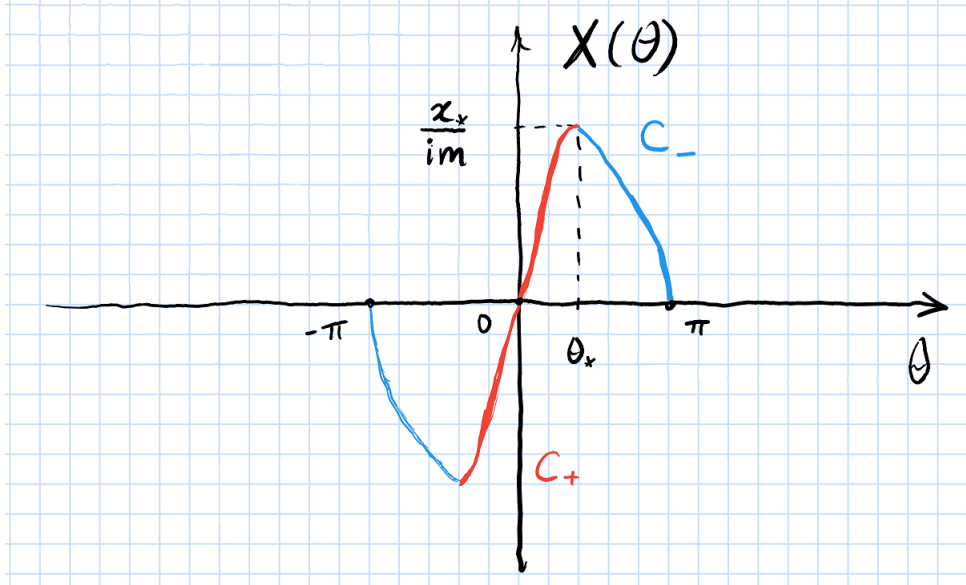
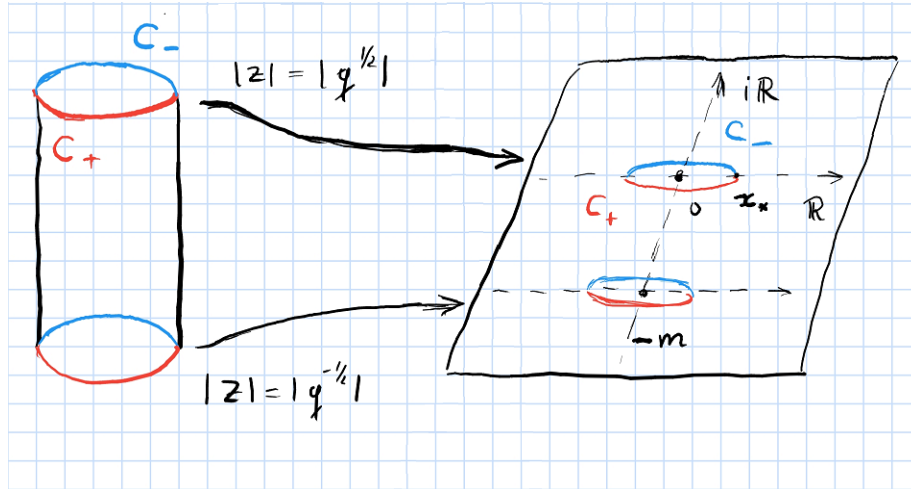
$$(62) \quad x_* := imX(\theta_*)$$

are the ends of the branch cut located on the real axis in the x -plane (see figure (4)). This means for any value of $x \in (-x_*, x_*)$ there are two corresponding values $\theta_{\pm}(x)$:

$$(63) \quad x = imX(\theta_+(x)) = imX(\theta_-(x))$$

We denote the upper side of the cut by C_+ , it is parametrized by θ running from $-\theta_*$ to θ_* . We denote the lower side of the cut by C_- , it is parametrized by θ running from $-\pi$ to $-\theta_*$, then from θ_* to π , see the figure (5). Therefore the jump which we are after is equal to:

$$(64) \quad i\pi m f''(x) = \frac{1}{F_{\mathfrak{q}}(\mathfrak{q}^{1/2} e^{i\theta_+})} - \frac{1}{F_{\mathfrak{q}}(\mathfrak{q}^{1/2} e^{i\theta_-})}.$$

FIGURE 4. $X(\theta)$ with colored sides of the cutFIGURE 5. Domain and image of $x(z)$

As

$$(65) \quad X'(\theta) = F_q(q^{1/2}e^{i\theta}) = -\frac{\wp\left(\frac{\tau}{2} + \frac{\theta}{2\pi}\right)}{4\pi^2},$$

the critical point θ_* is related to a zero of the Weierstrass function,. The latter has two zeroes on the elliptic curve, one giving the maximum of $X(\theta)$ for real θ , and the other the minimum. The Eq. (64) can be integrated once

to give:

$$(66) \quad f'(x) = \frac{\theta_+(x) - \theta_-(x)}{\pi} + 1$$

giving an elliptic version of arcsin law [6] of Vershik-Kerov. As the functions $\theta_+(x)$ and $\theta_-(x)$, so defined that they are continuous on the interval $(-x_*, x_*)$ with $\theta_+(x_*) = \theta_-(x_*)$ obey $\theta_-(-x_*) - \theta_+(-x_*) = 2\pi$, the choice of integration constant ensures $f'(x_*) = -f'(-x_*) = 1$ (cf. Fig. 5).

5. LIMITS AND ASYMPTOTICS

5.1. Edge asymptotics. The functions $\theta_{\pm}(x)$ are transcendental, but the edge behavior of $f''(x)$ is easy to analyze: as $x \rightarrow \pm x_*$, $\theta \rightarrow \theta_*$, and we can expand

$$(67) \quad X(\theta) = X(\theta_*) + \frac{1}{2}X''(\theta_*)(\theta - \theta_*)^2 + O((\theta - \theta_*)^3)$$

giving

$$(68) \quad \theta_{\pm} = \theta_* \pm \sqrt{\frac{2(x - x_*)}{imX''(\theta_*)}},$$

which by simple calculations leads to:

$$(69) \quad f''(x) \sim \frac{2}{\pi \sqrt{2imX''(\theta_*)(x - x_*)}} = \frac{\gamma}{\sqrt{x_* - x}}$$

with

$$(70) \quad \gamma = 2^{\frac{5}{4}} 3^{\frac{3}{4}} \pi^{-\frac{3}{2}} \left(1 - 504 \sum_{n=1}^{\infty} n^5 \frac{q^n}{1 - q^n} \right)^{-\frac{1}{4}}$$

We can compare (69) to (28):

$$(71) \quad f''_{VK}(x) \sim \frac{1}{\pi \sqrt{\Lambda}} \frac{1}{\sqrt{2\Lambda - x}}$$

Even though the functional forms of the edge asymptotics of the limit shapes in the elliptic and in the Vershik-Kerov case are similar, the detailed comparison requires a more precise matching of the parameters. We do this by taking the confluent (Inozemtsev) limit

$$(72) \quad m \rightarrow \infty, \quad q \rightarrow 0, \quad z \rightarrow 0$$

$$q^{1/2}m = -i\Lambda - \text{fixed}, \quad mz = y - \text{fixed}$$

In this limit the measure in (32) reduces to (6). Next, the only terms left in the product from the RHS of (42) are:

$$(73) \quad \left(1 - \frac{y}{Y(x)} \right) Y(x) \left(1 - y^{-1} \frac{\Lambda^2}{Y(x)} \right)$$

which is equal to:

$$(74) \quad \chi(x) - \left(y + \frac{\Lambda^2}{y} \right)$$

in agreement with the limit of (41). From (57) and (58) one sees that:

$$(75) \quad x(\mathfrak{q}^{1/2} e^{i\theta}) \rightarrow 2\Lambda \sin \theta$$

Hence, one has

$$(76) \quad \theta_+(x) = \vartheta_+^{VK} \left(\frac{x}{2\Lambda} \right) := \arcsin \frac{x}{2\Lambda}, \quad \theta_-(x) = \vartheta_-^{VK} \left(\frac{x}{2\Lambda} \right) := \pi - \arcsin \frac{x}{2\Lambda}$$

establishing the agreement between the Eqs. (66) and (30).

5.2. Matching the edge behaviour. The Inozemtsev limit of (69):

$$(77) \quad f''(x) \sim \frac{2}{\pi \sqrt{2imX''(\theta_*)(x-x_*)}} \rightarrow \frac{1}{\pi \sqrt{\Lambda(2\Lambda-x)}}$$

matches the edge behaviour of $f''_{VK}(x)$:

$$(78) \quad f''_{VK}(x) = \frac{1}{\pi\Lambda} \frac{1}{\sqrt{1 - \left(\frac{x}{2\Lambda}\right)^2}} \sim \frac{1}{\pi \sqrt{\Lambda(2\Lambda-x)}}$$

5.3. Expanding around Vershik-Kerov limir shape. The comparison of the limit shape of our problem to that of (6) is an instructive exercise in perturbative renormalization. Naively, fixing $\Lambda = im\mathfrak{q}^{\frac{1}{2}}$ and varying \mathfrak{q} , for small \mathfrak{q} we can find θ_* , $\theta_{\pm}(x)$ by expanding in $\mathfrak{q}^{\frac{1}{2}}$, cf. (76):

$$(79) \quad \theta_* = \frac{\pi}{2} - \mathfrak{q}^{\frac{1}{2}} \left(2 - \frac{8}{3}\mathfrak{q} + \frac{72}{5}\mathfrak{q}^2 - \frac{632}{7}\mathfrak{q}^3 + \frac{5462}{9}\mathfrak{q}^4 - \frac{47016}{11}\mathfrak{q}^5 + \dots \right),$$

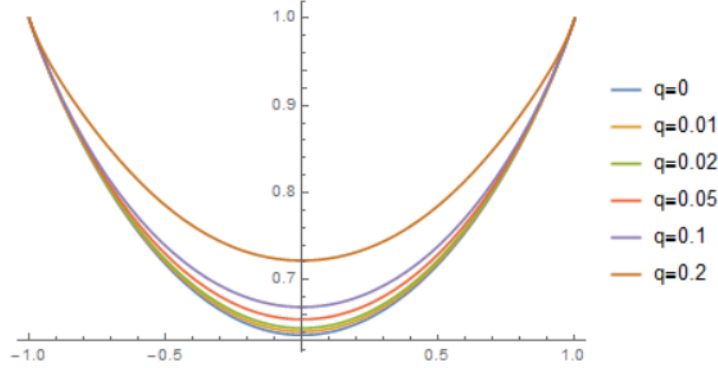
$$x_* = 2\Lambda (1 + 2\mathfrak{q} + 8\mathfrak{q}^3 - 29\mathfrak{q}^4 + 162\mathfrak{q}^5 + \dots),$$

which then leads to the naively singular expansion for $\theta_{\pm}(x)$ and $f(x)$:

$$(80) \quad \theta_{\pm}(x) \stackrel{?}{=} \vartheta_{\pm}^{VK}(\xi) - 2\mathfrak{q}^{\frac{1}{2}}\xi \mp 2\mathfrak{q} \frac{\xi^3}{\sqrt{1-\xi^2}} + 4\mathfrak{q}^{\frac{3}{2}}\xi \left(1 + \frac{2}{3}\xi^2 \right) + O(\mathfrak{q}^2),$$

$$f'(x) \stackrel{?}{=} \frac{2}{\pi} \arcsin \xi - \frac{4\mathfrak{q}}{\pi} \frac{\xi^3}{\sqrt{1-\xi^2}} + O(\mathfrak{q}^2),$$

with $\xi = x/2\Lambda$. There are, of course, no singular terms in $f'(x)$, as it is a monotone continuous function on $[-x_*, x_*]$, changing from -1 to $+1$. The resolution of the puzzle is that the singularities reflect the \mathfrak{q} -dependence of


 FIGURE 6. $f(x)$ to the first few orders in q

the cut. If instead of Λ one keeps fixed x_* , the corresponding expansion becomes perfectly non-singular:

$$(81) \quad \theta_{\pm}(x) = \vartheta_{\pm}^{VK}(y) - 2q^{\frac{1}{2}}y \times \\ (1 - \frac{4q}{3}y^2 + 4q^2(1 - 2y^2 - \frac{4}{5}y^4) - 20q^3(1 + \frac{2}{5}y^2 - \frac{16}{5}y^4 - \frac{16}{35}y^6) + 61q^4(1 + \frac{272}{61}y^2 - \frac{224}{61}y^4 - \frac{384}{61}y^6 - \frac{256}{549}y^8) + \dots) + \\ \mp 2qy\sqrt{1-y^2} \times \\ (1 - 3q(1 + \frac{2}{3}y^2) + 6q^2(1 + \frac{40}{9}y^2 + \frac{8}{9}y^4) - 3q^3(1 + 38y^2 + 56y^4 + \frac{16}{3}y^6) + \frac{7296}{5}q^4y^4(1 + \frac{12}{19}y^2 + \frac{2}{57}y^4) + \dots),$$

where $y = x/x_*$. For the values of $q = 0, 0.01, 0.02, 0.05, 0.1, 0.2$ and $x_* = 1$ the plot of function $f(x)$ is drawn in the figure (6).

6. CONCLUSIONS AND FUTURE DIRECTIONS

In this paper we explored a one-parametric deformation $\mu_{m,q,\hbar}$ of the Plancherel measure on the set of Young diagrams, and found its limit shape. Specifically, we kept the size fugacity q finite, and tuned the parameter $m/\hbar \rightarrow \infty$.

There is a natural generalization of such limit shape problem (motivated, e.g. by topological string theory and gauge theory [15, 9]), where the measure $\mu[\lambda]$ includes the chemical potentials for the generalized Casimirs \mathbf{p}_k . Introduce the sequence (t_k) , $k = 1, 2, \dots$ of formal variables, the formal function

$$(82) \quad \mathbf{t}(x) = \sum_{k=1}^{\infty} t_k x^k$$

and define the measures (cf. [9])

$$(83) \quad \mu_{\Lambda, \hbar; \mathbf{t}}[\lambda] = \mu_{\Lambda, \hbar}[\lambda] e^{\mathbf{t}(hc_{\square})} \\ \mu_{m, q, \hbar; \mathbf{t}}[\lambda] = \mu_{m, q, \hbar}[\lambda] e^{\mathbf{t}(hc_{\square})}$$

The limit shape is now governed by the analytic multi-valued function $Y(x)$, which behaves as $x + o(x^{-1})$ on the physical sheet, such that, in the first case,

$$(84) \quad Y(x) + \Lambda^2 \frac{e^{\mathbf{t}(x)}}{Y(x)}$$

is an entire function of x . One cannot claim (84) is a linear function of x , as the LHS has an essential singularity at $x \rightarrow \infty$. However, the formal nature of variables t_k suggests the Riemann surface of Y is still a two-sheeted cover of the x -plane. Also, the probabilistic nature of the problem shows Y has a single cut on the physical sheet. By comparing the two terms in the LHS of (84) one concludes Y is an analytic function on the curve \mathcal{C}

$$(85) \quad y + \frac{\tilde{\Lambda}^2}{y} = x + \tilde{v}$$

where the parameters $(\tilde{v}, \tilde{\Lambda})$ are the formal functions of t_k , such that at $t_k = 0$ they approach $(0, \Lambda)$. There are two special points P_{\pm} , where $x = \infty$. At P_+ , $y \sim x$ and at P_- , $y \sim \Lambda^2 x^{-1} \rightarrow 0$. In other words $(x, y) = (\infty, \infty)$ at P_+ , and $(x, y) = (\infty, 0)$ at P_- . The function Y is found from the following conditions: it is holomorphic on \mathcal{C} outside P_{\pm} , and it has the asymptotics

$$(86) \quad \begin{aligned} Y &\sim x, (x, y) \rightarrow P_+, \\ Y &\sim \Lambda^2 x^{-1} e^{\mathbf{t}(x)}, (x, y) \rightarrow P_- \end{aligned}$$

Here is how one finds such a function: Define the functions Ω_k^{\pm} to be meromorphic functions on \mathcal{C} , holomorphic outside P_{\pm} , respectively, such that

$$(87) \quad \Omega_k^{\pm} = x^k + o(x^{-1}), (x, y) \rightarrow P_{\pm} .$$

It follows

$$(88) \quad x^k = \Omega_k^+(y) + \Omega_k^-(y) - \omega_k ,$$

where

$$(89) \quad \omega_k = \Omega_k^+(P_-) = \Omega_k^-(P_+) = \frac{1}{2\pi i} \oint_{|y|=|\tilde{\Lambda}|} \frac{dy}{y} x^k .$$

Then

$$(90) \quad Y = y \exp \sum_k t_k (\Omega_k^-(y) - \omega_k)$$

has the correct asymptotics both at P_{\pm} , and continues analytically across the cuts of the y -function, provided that the matching equations at the branch-points

$$(91) \quad \tilde{\Lambda}^2 e^{-\sum_k t_k \omega_k} = \Lambda^2$$

hold and the vanishing period

$$(92) \quad 0 = - \oint x \frac{dY}{Y} = \tilde{v} + \sum_k t_k \text{Coeff}_{y^{-1}} \Omega_k^-$$

guarantees the correct asymptotics $Y \sim x + o(x^{-1})$ on the physical sheet. This gives two equations for the two unknowns $(\tilde{v}, \tilde{\Lambda})$. For example, setting $t_2 = t_3 = \dots = 0$ one easily recovers the Lambert solution found in [10]:

$$(93) \quad \tilde{v} = -t_1 \tilde{\Lambda}^2, \quad \Lambda^2 = \tilde{\Lambda}^2 e^{-2t_1 \tilde{\Lambda}^2}$$

with its finite convergence radius typical of Whitham hierarchies [7]. The second case of (83) and other generalizations will be presented in the companion paper [5].

There is yet another class of limit shape problems, where the parameter m/\hbar in $\mu_{m, \mathbf{q}, \hbar}$ is fixed while the instanton fugacity \mathbf{q} approaches 1, a Hardy-Ramanujan limit. In the special case of $m = 0$, the limit shape curve is the celebrated

$$(94) \quad e^{-a} + e^{-b} = 1, \quad a, b \geq 0$$

The generalizations to $m \neq 0$ will be considered elsewhere.

Finally, all the measures discussed above were symmetric under $\lambda \mapsto \lambda^t$. Four dimensional gauge theory [12] suggests yet another natural generalization, in which the weight of the box $\square \in \lambda$ depends separately on the arm $a_\square = \lambda_i - j$ and the leg $l_\square = \lambda_j^t - i$, for example

$$(95) \quad \mu_{m, \mathbf{q}; \varepsilon_1, \varepsilon_2}[\lambda] = \frac{1}{Z_{2^*}(m, \mathbf{q}; \varepsilon_1, \varepsilon_2)} \mathbf{q}^{|\lambda|} \times \prod_{\square} \left(1 + \frac{m}{\varepsilon_1(a_\square + 1) - \varepsilon_2 l_\square} \right) \left(1 + \frac{m}{-\varepsilon_1 a_\square + \varepsilon_2(l_\square + 1)} \right)$$

Of course, such measures are well-known to mathematicians under the name of discrete β -ensembles, Jack processes, etc. [1, 2]. We know [13] the partition function exponentiates

$$(96) \quad Z_{2^*}(m, \mathbf{q}; \varepsilon_1, \varepsilon_2) \sim \exp \frac{1}{\varepsilon_2} W(m, \mathbf{q}; \varepsilon_1)$$

when $\varepsilon_2 \rightarrow 0$ with $m, \varepsilon_1, \mathbf{q}$ kept constant. The corresponding limit shape is described by a quantum spectral curve [4].

Acknowledgements. We have greatly benefited from patient explanations of I. Krichever and A. Okounkov. Research is partly supported by NSF PHY Award 2310279.

7. APPENDIX. PROOF OF THE FACTORIZATION FORMULA

The $\hbar \rightarrow 0$ limit of the normalized qq -character, including the higher times, is given by

$$(97) \quad \chi(x) = \phi(\mathbf{q}) \sum_{\lambda} \mathbf{q}^{|\lambda|} \prod_{\square \in \lambda} e^{t(x + mc_\square)} \frac{\prod_{\square \in \partial_+ \lambda} Y(x + mc_\square)}{\prod_{\square \in \partial_- \lambda} Y(x + mc_\square)}$$

Motivated by [4] we prove the following **Lemma**: Let z be an indeterminate. The following identity holds:

$$(98) \quad Y(x) \cdot \prod_{n=0}^{\infty} \left(1 - zq^n e^{\hat{t}(x+mn)} \frac{Y(x+(n+1)m)}{Y(x+nm)} \right) \times \\ \prod_{n=1}^{\infty} \left(1 - z^{-1}q^n e^{-\hat{t}(x-nm)} \frac{Y(x-nm)}{Y(x-(n-1)m)} \right) = \\ \sum_{n=1}^{\infty} (-z)^n q^{\frac{n^2-n}{2}} e^{\sum_{j=0}^{n-1} \hat{t}(x+jm)} \chi(x+nm) + \chi(x) + \\ + \sum_{n=1}^{\infty} (-z)^{-n} q^{\frac{n^2+n}{2}} e^{-\sum_{j=1}^n \hat{t}(x-jm)} \chi(x-nm)$$

where $\hat{t}(x)$ a unique formal power series in x , $\hat{t}(0) = 0$, solving:

$$(99) \quad t(x) = \hat{t}(x) - \hat{t}(x-m)$$

Proof. \square By a simple cancellation of factors the formula for the qq -character could be rewritten as:

$$(100) \quad \chi(x) = \sum_{\lambda} q^{|\lambda|} \prod_{\square \in \lambda} e^{t(x+m_{\square})} \prod_{j=1}^{\lambda_1} \frac{Y(x+m(\lambda_j^t-j+1))}{Y(x+m(\lambda_j^t-j))} Y(x-m\lambda_1)$$

Opening the brackets in the LHS of the formula (98) one obtains:

$$(101) \quad \sum_{\substack{r,s \geq 0 \\ n_0 > n_1 > \dots > n_{r-1} \geq 1 \\ 0 \leq k_0 < k_1 < \dots < k_{s-1}}} (-z)^{r-s} \prod_{i=0}^{r-1} q^{n_i-1} e^{\hat{t}(x+(n_i-1)m)} \prod_{i=0}^{s-1} q^{k_i+1} e^{-\hat{t}(x-(k_i+1)m)} \\ \cdot \prod_{i=0}^{r-1} \frac{Y(x+n_i m)}{Y(x+(n_i-1)m)} \cdot Y(x) \cdot \prod_{i=0}^{s-1} \frac{Y(x-(k_i+1)m)}{Y(x-k_i m)}$$

Note that the two sets of strictly increasing numbers $n_0 > n_1 > \dots > n_{r-1} \geq 1$ and $0 \leq k_0 < k_1 < \dots < k_{s-1}$ encode the information about a Young diagram λ and an additional integer, which could be interpreted as a shift of the Young diagram perpendicular to the main diagonal. The dictionary is the following. The shift is equal to $p = r - s$. The positive integers n_j define the lengths of the first r -columns, and k_i define the length of the first s -rows, through the formulas:

$$(102) \quad n_j = \lambda_{j+1}^t - j + p, \quad j = 0, \dots, r-1$$

$$(103) \quad k_{s-i} = \lambda_i - i - p, \quad i = 1, \dots, s$$

This data uniquely determines the diagram. Notice that, given λ and p the numbers r and s are uniquely determined as such values of i and j where

the expressions $\lambda_i - i - p$, $\lambda_{j+1}^t - j + p$ change sign. With this substitution the above expression could be rewritten as follows:

$$(104) \quad \sum_{p \in \mathbb{Z}} \sum_{\lambda} (-z)^p \prod_{j=0}^{r-1} q^{\lambda_{j+1}^t - j + p - 1} e^{\hat{t}(x + m(\lambda_{j+1}^t - j + p - 1))} \times \\ \prod_{i=1}^s q^{\lambda_i - i - p + 1} e^{\hat{t}(x + m(\lambda_i - i - p + 1))} \times Y(x) \times \\ \prod_{j=0}^{r-1} \frac{Y(x + (\lambda_{j+1}^t - j + p)m)}{Y(x + (\lambda_{j+1}^t - j + p - 1)m)} \times \prod_{i=1}^s \frac{Y(x - (\lambda_i - i - p + 1)m)}{Y(x - (\lambda_i - i - p)m)}$$

Now we need to match every multiple in the product to every multiple in the expression (100), shifted by p . Let us denote:

$$(105) \quad \text{LHS}(\lambda, p) = \prod_{j=0}^{r-1} \frac{Y(x + (\lambda_{j+1}^t - j + p)m)}{Y(x + (\lambda_{j+1}^t - j + p - 1)m)} \cdot Y(x) \cdot \prod_{i=1}^s \frac{Y(x - (\lambda_i - i - p + 1)m)}{Y(x - (\lambda_i - i - p)m)} \\ \text{RHS}(\lambda, p) = Y(x - m(\lambda_1 - p)) \prod_{j=1}^{\lambda_1} \frac{Y(x + m(\lambda_j^t - j + 1 + p))}{Y(x + m(\lambda_j^t - j + p))}$$

We are going to prove that $\text{LHS}(\lambda, p) = \text{RHS}(\lambda, p)$ by induction on the number of boxes in the Young diagram.

The base of the induction is the case when $\lambda = \emptyset$, and either $r = 0$, and hence $s = -p$, or $s = 0$, and $r = p$.

Let us consider the case $r = 0$ first. The $\text{LHS}(\emptyset, -s)$ of the formula above then takes the form:

$$(106) \quad Y(x) \cdot \prod_{i=1}^s \frac{Y(x + (i + p - 1)m)}{Y(x + (i + p)m)}$$

which is, after cancelling all factors, is equal to the $\text{RHS}(\emptyset, -s) = Y(x + mp)$. Letting now $s = 0$, one has:

$$(107) \quad \text{LHS}(\emptyset, r) = \\ = \prod_{j=0}^{r-1} \frac{Y(x + (r - j)m)}{Y(x + (r - j - 1)m)} Y(x - (r - 1)) = Y(x + rm)$$

which is equal to the $\text{RHS}(\emptyset, r)$.

For the induction step, let us assume, that we are adding one box to the k 'th row. For the LHS the cases $k - \lambda_k - 1 + p \geq 0$ and $k - \lambda_k - 1 + p < 0$ should be treated separately, because they affect the product of the first r factors or the last s factors correspondingly, but eventually the final result

is the same:

$$(108) \quad \frac{\text{LHS}(\lambda + 1_k, p)}{\text{LHS}(\lambda, p)} = \frac{Y(x - (\lambda_k - k - p + 2)m)}{Y(x - (\lambda_k - k - p + 1)m)} \frac{Y(x - (\lambda_k - k - p)m)}{Y(x - (\lambda_k - k - p + 1)m)}$$

By analogous calculation same is for the RHS. Hence the formula is proven. Now let us deal with the factors depending on $\hat{t}(x)$. In the LHS we have the function in the exponent:

$$(109) \quad d(\lambda, p) := \sum_{i=0}^{r-1} \hat{t}(x + m(n_i - 1)) - \sum_{j=0}^{s-1} \hat{t}(x - m(k_j + 1))$$

Similarly to the discussion above we could calculate its change under the addition of the box into the k 's row:

$$(110) \quad d(\lambda + 1_k, p) - d(\lambda, p) = \hat{t}(x - m(\lambda_k - k - p + 1)) - \hat{t}(x - m(\lambda_k - k - p + 2))$$

For the RHS we would like to look at the function:

$$(111) \quad d'(\lambda, p) := \sum_{\square \in \lambda} t(x + m(p + c_{\square})) = \sum_{\square \in \lambda} \hat{t}(x + m(p + c_{\square})) - \hat{t}(x + m(p - 1 + c_{\square}))$$

And hence:

$$(112) \quad d'(\lambda + 1_k, p) - d'(\lambda, p) = \hat{t}(x - m(\lambda_k - k - p + 1)) - \hat{t}(x - m(\lambda_k - k - p + 2))$$

So the step of the induction is proven. And for the base we have:

$$(113) \quad d'(\emptyset, p) = 0$$

However:

$$(114) \quad d(\emptyset, p) = \begin{cases} \sum_{j=0}^{p-1} \hat{t}(x + jm), & p \geq 0 \\ -\sum_{j=1}^{-p} \hat{t}(x - jm), & p < 0 \end{cases}$$

exactly the factors we see in (98). The last step is to compare the \mathfrak{q} dependence. This proof is carried out by the same trick.

Note that the proof is similar to fermionic proof of Jacobi triple product identity. ■

REFERENCES

- [1] A. Borodin, G. Olshanski, *z-measures on partitions and their scaling limits*, arXiv e-prints. doi:10.48550/arXiv.math-ph/0210048
- [2] E. Dimitrov, and A. Knizel, *Asymptotics of discrete β -corners processes via two-level discrete loop equations*, Probability and Mathematical Physics 3.2 (2022): 247-342.
- [3] R. Donagi and E. Witten, *Supersymmetric Yang-Mills theory and integrable systems*, Nucl. Phys. B **460**, 299-334 (1996) doi:10.1016/0550-3213(95)00609-5 [arXiv:hep-th/9510101 [hep-th]].
- [4] A. Grekov, N. Nekrasov, *Elliptic Calogero-Moser system, crossed and folded instantons, and bilinear identities*, (2023) arXiv:2310.04571 [math-ph]
- [5] A. Grekov, N. Nekrasov, *Vershik-Kerov in higher times and higher spaces*, to appear.

- [6] S. Kerov and A. Vershik, *Asymptotics of the Plancherel measure of the symmetric group and the limiting form of Young tableaux*, Doklady akademii nauk, Russian Academy of Sciences Vol. **233** (1977) 6, pp. 1024-1027, MR0480398
- [7] I. Krichever, *The τ -function of the universal Whitham hierarchy, matrix models and topological field theories*, Commun. Pure Appl. Math. **47**, 437 (1994) [[arXiv:hep-th/9205110](#)] [hep-th].
- [8] B. Logan and L. Shepp, *A variational problem for random Young tableaux*, Adv.Math. **26** (1977) 206-222, MR1417317
- [9] A. S. Losev, A. Marshakov and N. A. Nekrasov, *Small instantons, little strings and free fermions*, [[arXiv:hep-th/0302191](#)] [hep-th].
- [10] A. Marshakov and N. Nekrasov, *Extended Seiberg-Witten Theory and Integrable Hierarchy*, JHEP **01**, 104 (2007) doi:10.1088/1126-6708/2007/01/104 [[arXiv:hep-th/0612019](#)] [hep-th].
- [11] N. Nekrasov and A. Okounkov, *Seiberg-Witten theory and random partitions*, In, 'The Unity of Mathematics: In Honor of the Ninetieth Birthday of I.M. Gelfand', Boston, MA: Birkhäuser Boston (2006) 525-596.
- [12] N. A. Nekrasov, *Seiberg-Witten prepotential from instanton counting*, Adv. Theor. Math. Phys. **7**, no.5, 831-864 (2003) doi:10.4310/ATMP.2003.v7.n5.a4 [[arXiv:hep-th/0206161](#)] [hep-th].
- [13] N. Nekrasov, *BPS/CFT correspondence: non-perturbative Dyson-Schwinger equations and qq-characters*, Journal of High Energy Physics, **3** (2016) 1-70
- [14] N. Nekrasov, V. Pestun, *Seiberg-Witten Geometry of Four-Dimensional $N = 2$ Quiver Gauge Theories*, [arXiv:1211.2240v2](#) [hep-th]
- [15] A. Okounkov, and R. Pandharipande, *Gromov-Witten theory, Hurwitz theory, and completed cycles*, (2002) [arXiv:0204305](#) [math.AG]
- [16] C. Vafa and E. Witten, *A Strong coupling test of S duality*, Nucl. Phys. B **431**, 3-77 (1994) doi:10.1016/0550-3213(94)90097-3

SIMONS CENTER FOR GEOMETRY AND PHYSICSⁿ, YANG INSTITUTE FOR THEORETICAL PHYSICS^{g,n}, STONY BROOK UNIVERSITY, STONY BROOK NY 11794-3636, USA